

# KIRTLANDIA

The Cleveland Museum of Natural History

December 2007

Number 56:65–71

## <sup>40</sup>AR/<sup>39</sup>AR DATING OF THE LEMUDONG'O LATE MIOCENE FOSSIL ASSEMBLAGES, SOUTHERN KENYA RIFT

ALAN L. DEINO

Berkeley Geochronology Center  
2455 Ridge Road  
Berkeley, California 94709

AND STANLEY H. AMBROSE

Department of Anthropology  
University of Illinois, 109 Davenport Hall, 607 S. Matthews Ave.  
Urbana, Illinois 61801-3636

### ABSTRACT

The Messinian (uppermost Miocene) Lemudong'o Formation in Lemudong'o Gorge, near the western edge of the southern Kenya Rift, contains fine-grained tuffs stratified below and within fossil-bearing mudstones deposited along an intermittently exposed paleolake margin. This site has yielded a diverse fauna including colobine monkeys, carnivores, and other large land animals, as well as micromammals and seeds. Single-crystal laser-fusion <sup>40</sup>Ar/<sup>39</sup>Ar ages from three tuffs underlying the fossil-bearing horizon are  $6.087 \pm 0.013$ ,  $6.10 \pm 0.03$ , and  $6.12 \pm 0.07$  Ma. One tuff interstratified with the fossiliferous deposits yielded an age of  $6.084 \pm 0.019$  Ma. The narrow analytical spread of these ages suggests rapid deposition of the section and relatively little habitat averaging of the fossil assemblage. Lemudong'o affords a snapshot of Miocene stratigraphy and paleontology in a region of Kenya dominated by Plio-Pleistocene rocks.

### Introduction

Lemudong'o is a late Miocene paleontological site in the Ewaso Ng'iro River valley above the western edge of the southern Kenya Rift Valley, approximately 30 km south of Narok town (Figure 1) (Kyule et al., 1997; Ambrose et al., 2002; Hlusko et al., 2002; Ambrose et al., 2003; Haile-Selassie et al., 2004; Ambrose, Bell, et al., 2007; Ambrose, Kyule, and Hlusko, 2007; Ambrose, Nyamai, et al., 2007). The site occurs stratigraphically within the Lemudong'o Formation, a widely exposed (25 × 50 km) sequence of deeply incised lavas, tuffs, lacustrine, fluvial and alluvial sediments, and paleosols of middle Miocene to Late Pleistocene age (Wright, 1967; Crossley, 1979). The geology and paleoecology of the site and vicinity are summarized below, followed by details of the <sup>40</sup>Ar/<sup>39</sup>Ar geochronology, and brief discussion of the implications of the age of the Lemudong'o fauna for understanding the origins of Mio-Pliocene hominids.

### Geology, Stratigraphy, Paleontology, and Paleoecology

Details of the history of research, and the geology, paleontology and paleoecology of the Lemudong'o Formation are described elsewhere (Ambrose, Bell, et al., 2007; Ambrose, Kyule, and Hlusko, 2007; Ambrose, Nyamai, et al., 2007). Wright (1967) reconstructed three overlapping ancient lake basins in the southern Narok region that he considered to be of Plio-

Pleistocene age. Crossley (1979) and Waibel and McDonough (1977) subsequently reported whole-rock K/Ar dates for some of the lavas and tuffs in this region, spanning the middle Miocene to early Pliocene (15–4 Ma). Deposits of Wright's second paleolake basin comprise the Lemudong'o Formation (Ambrose, Nyamai, et al., 2007).

The Lemudong'o Formation comprises a stratified sequence of sediments and tuffs up to 135-m thick (Ambrose, Nyamai, et al., 2007). The base of the formation lies unconformably on a variety of rock types, including Neoproterozoic metamorphic rocks, and Miocene volcanic rocks including basalts, phonolites, and welded ignimbrites. The top of the formation contains a waterlain yellow tuff that is everywhere conformably overlain by a gray ignimbrite. In the eastern part of the paleobasin, encompassing Lemudong'o, a thick blue-gray trachyte lava caps the succession.

Three main phases of sedimentation have been provisionally defined in the Lemudong'o Formation (Ambrose, Nyamai, et al., 2007). Phase 1 comprises predominantly claystones, silty and sandy claystones (mudstones), laminated siltstones and thin, discontinuous beds of sandstones, fine gravels and tufas. Depositional environments are dominantly lacustrine, swamp and lake margin, with occasional small, low-energy streams. The tuffs dated in this study lie within the upper half of this depositional phase. Phase 2 comprises poorly sorted clayey and silty sandstones in the Lemudong'o area, representing distal alluvial-

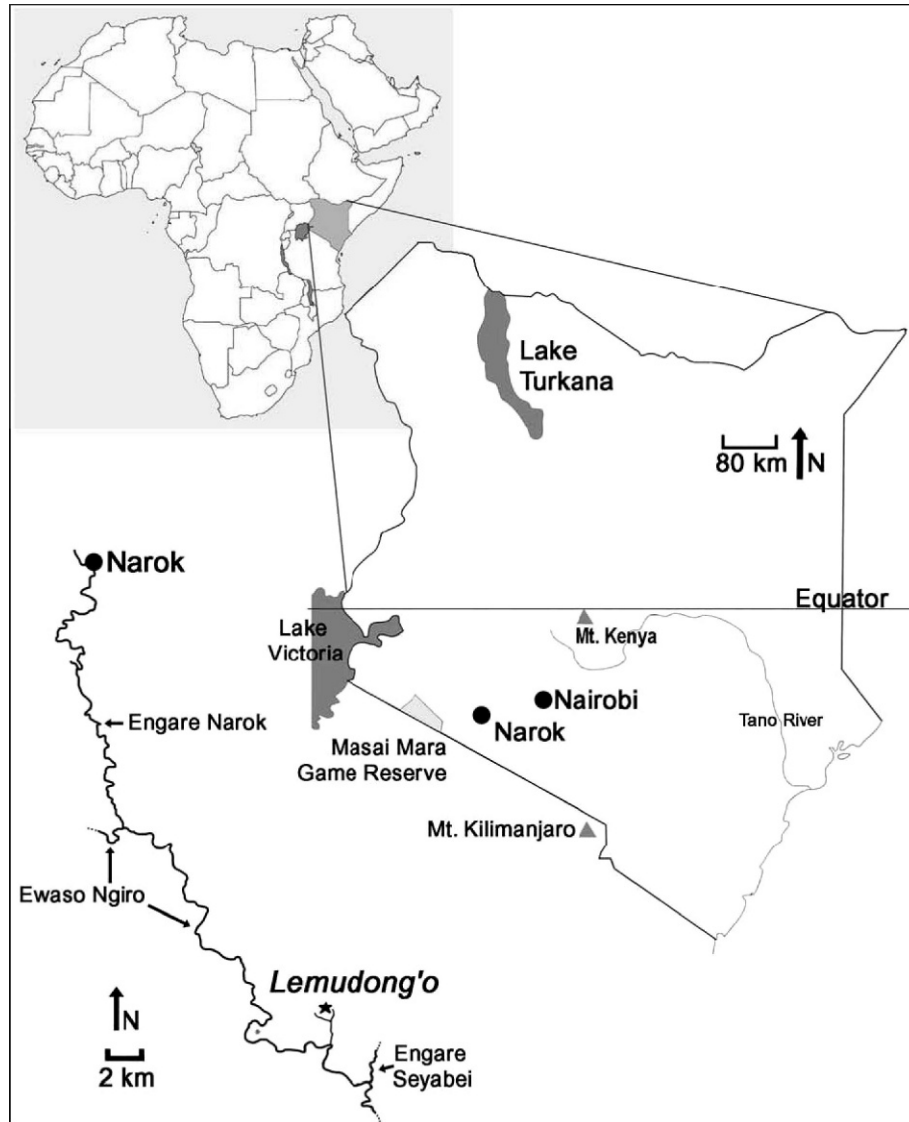


**Figure 1.** Location of the Lemudong'o paleontological site, southern Kenya Rift Valley.

and colluvial-fan deposition near the paleobasin margin, and paleosols formed on well-sorted silts in the basin center. Phase 3 comprises laminated siltstones, tuffs and ignimbrites, marking a return to lacustrine deposition. This lacustrine phase was terminated by a massive pyroclastic eruption.

The most productive paleontological areas at Lemudong'o (Figure 2) are exposed in the upper reaches of the main gully at Locality 1 (GvJh15 at  $1^{\circ} 18.19' S$ ,  $35^{\circ} 58.74' E$ ). The main outcrops of Locality 2 (GvJh32), exposed  $\sim 500$  m south in the Lemudong'o Gorge at  $1^{\circ} 17.98' S$ ,  $35^{\circ} 59.04' E$ , have no diagnostic fossils (Ambrose et al., 2003; Ambrose, Kyule, and Hlusko, 2007; Ambrose, Nyamai, et al., 2007). Locality 1 has two main fossil assemblages. The upper assemblage occurs in a 6-m-thick bed of silty to sandy clayey mudstones (Figure 2), representing near-shore lacustrine, swamp, and intermittently exposed lakeshore depositional environments. Colobine monkeys, hyrax, small carnivores, and bovids dominate the faunal assemblage. The upper mudstones enclose one of the dated tuffs (the "speckled tuff"), which itself contains fossil vertebrates and plants, including micromammals and seeds of the equatorial forest tree

*Celtis zenkeri* (Ambrose et al., 2003). The floral and faunal habitat preferences suggest a mesic forest habitat (Ambrose, Bell, et al., 2007).

The lower fossil assemblage at Locality 1 is derived from coarse sandstone, clayey sandstone, and well-sorted fine gravel directly underlying the claystone and above a bed of laminated yellow siltstones. This higher energy depositional environment is provisionally attributed to a moderately high-energy regressive-shoreline beach deposit. It contains rolled fragments of semi-aquatic animals such as hippopotamus and crocodile, and terrestrial mammals including colobine primates, hyrax, bovids, proboscideans (*Anancus*), mustelid carnivores (*Plesiogulo*), suids (*Nyanzachoerus syrticus*), and hyenas. These lower sandstones also contain an undated, thin, lenticular bed of fine-grained dark-green tuff (Figure 2).

Localities 1 and 2 are correlated by the lateral continuity of the key rock units, including the lacustrine silts and the yellow tuff, gray ignimbrite, and blue-gray trachyte at the top of both sections. The base of the sedimentary sequence at Locality 1 exposes the top meter of a thick bed of mudstones below the

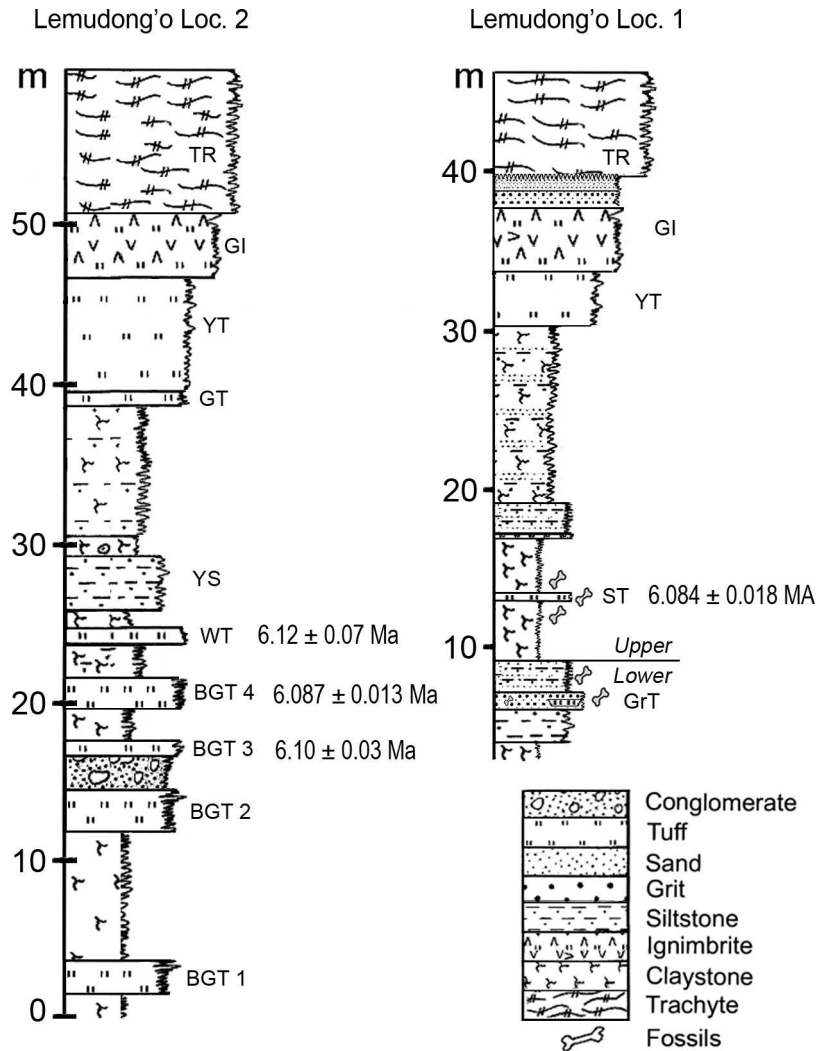


**Figure 2.** Stratigraphic sections for Lemudong'o Localities 1 and 2, showing  $^{40}\text{Ar}/^{39}\text{Ar}$  age results from dated tuff samples. The boundary between fossil assemblages from upper mudstone and lower coarse-grained deposits is indicated. Abbreviations for strata: BGT1-4, blue-gray tuffs 1-4; WT, white tuff; YS, yellow laminated lacustrine silts; GrT, green tuff; ST, speckled tuff; GI, gray ignimbrite; YT, tellow tuff; TR, trachyte lava.

lacustrine siltstones. The sequence at Locality 2 extends substantially deeper into older strata, and contains five stratified tuffs below the lacustrine siltstones that afford an opportunity to precisely establish the age of the fossil assemblages through  $^{40}\text{Ar}/^{39}\text{Ar}$  dating. The four lowest of these tuffs are lithologically similar: light blue-gray in color, massive to weakly laminated, and fine-grained. Similar tuffs occur in outcrops between the lower Lemudong'o channel and the east side of Enemankeon.

#### $^{40}\text{Ar}/^{39}\text{Ar}$ Dating

Anorthoclase phenocrysts were extracted for single-crystal, laser-fusion  $^{40}\text{Ar}/^{39}\text{Ar}$  age determination from four separate tuffs: the "speckled tuff" in mudstones above the main lacustrine siltstone in Locality 1 (sample GvJh15), and three tuffs below the lacustrine siltstone in Locality 2 (from bottom to top, samples GvJh32-8, -6 and -4) (Figure 2). The speckled tuff is stratified within clayey mudstones. Locality 2 dated tuffs are all weakly laminated, quiet-water deposits without obvious detrital contamination in outcrop. The speckled and the upper blue-gray tuffs

(BGT4) from Locality 2 contain moderately coarse K-feldspar up to a few mm in size, while feldspars in the other tuffs are finer grained, relatively rare, and proved difficult to date.

Samples were prepared by gentle crushing and sieving to extract the 0.35–1.2 mm size fraction of bulk tuff. K-feldspar (anorthoclase) phenocrysts were concentrated using magnetic and occasionally heavy-liquid separation techniques. The mineral separates were then treated with dilute HCl, HF, and distilled water in an ultrasonic bath to remove adhered matrix, and then hand-selected to obtain pristine, inclusion-free feldspars.

The anorthoclase crystal concentrates were irradiated in two batches in the Cd-lined, in-core CLICIT facility of the Oregon State University TRIGA reactor. Sample GvJh15 received 7 hours of irradiation while the other three samples received 2 hours. Sanidine from the Fish Canyon Tuff of Colorado was used as a mineral standard, with a reference age of 28.02 Ma (Renne et al., 1998).

$^{40}\text{Ar}/^{39}\text{Ar}$  extractions were performed at the Berkeley Geochronology Center (BGC), using a focused  $\text{CO}_2$  laser to fuse and

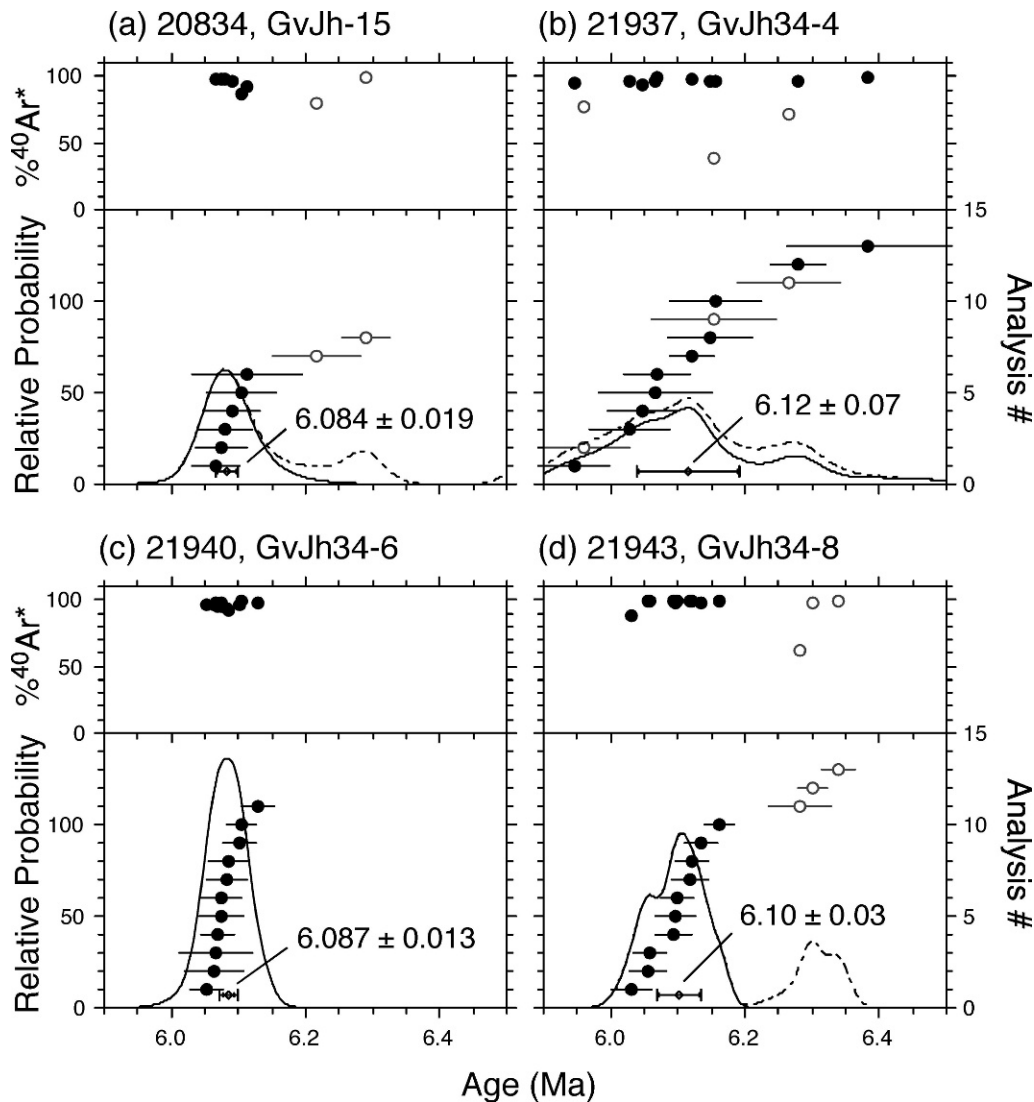


**Figure 3.** Age-probability density diagrams for the single-crystal,  $^{40}\text{Ar}/^{39}\text{Ar}$  dating results. Open circles represent analyses omitted from the weighted-mean age (shown toward the bottom of each diagram). Dashed curve is the relative probability calculated with all samples included; the solid line is without the omitted analyses.

rapidly liberate trapped argon from individual feldspar crystals. Gasses were scrubbed with SAES getters for several minutes to remove impurities ( $\text{CO}$ ,  $\text{CO}_2$ ,  $\text{N}_2$ ,  $\text{O}_2$ , and  $\text{H}_2$ ), followed immediately by measurement of the purified noble gases for five argon isotopes on a MAP 215-50 mass spectrometer for approximately 30 minutes. From 9 to 13 grains were analyzed per sample, totaling 46 single-crystal age determinations. See Deino and Potts, 1990, Best et al., 1995, and Deino et al., 1998 for additional details regarding the  $^{40}\text{Ar}/^{39}\text{Ar}$  dating method and its implementation at BGC.

### Results

Full analytical results for the  $^{40}\text{Ar}/^{39}\text{Ar}$  determinations are listed in Table 1, and summarized in Table 2. All but a few crystals yielded high proportions of radiogenic ( $^{40}\text{Ar}^*$ ) to atmospheric  $^{40}\text{Ar}$ , as would be expected for unaltered, inclusion-free K-feldspars of this age. Several exhibited markedly lower percentages of  $^{40}\text{Ar}^*$ , likely reflecting the presence of small

inclusions, trapped pockets of atmosphere, incipient alteration, etc. An arbitrary cutoff of 80%  $^{40}\text{Ar}^*$  was employed to cull anomalous grains, which were then excluded from further data analysis (5 of 46 analyses). A further four grains were omitted because they were “obviously” too old—i.e., clearly separated in the primary mode on age-probability diagrams (Figure 3).

As illustrated by the age-probability diagrams and demonstrated by population statistics (Table 2), samples GvJh15 and GvJh32-6 yielded unimodal, nearly symmetrical distributions with low MSWD's (0.12 to 1.49, respectively). These distributions are interpreted as representing undisturbed isotopic systematics from a single population of primary volcanic feldspars. They yield weighted-mean ages of  $6.084 \pm 0.019$  (1 $\sigma$  standard error, including error in  $J$ , the neutron fluence calibration parameter) and  $6.087 \pm 0.013$ . Samples GvJh32-4 and -8, in contrast, yielded broader, multimodal distributions with high MSWD's ( $> 5$ ) indicating greater scatter in the age distribution than can be explained by the estimated analytical errors alone. Thus, these

Table 1.  $^{40}\text{Ar}/^{39}\text{Ar}$  analytical results.

Lab ID no.	Relative isotopic abundances										Derived results						
	$^{40}\text{Ar}$		$^{39}\text{Ar}$		$^{38}\text{Ar}$		$^{37}\text{Ar}$		$^{36}\text{Ar}$		$^{39}\text{Ar Mol}$	Ca/K	$\%^{40}\text{Ar}^*$	Age (Ma)	w/ $\pm$ J		
	$\pm 1\sigma$		$\pm 1\sigma$	$\pm 1\sigma$		$\pm 1\sigma$		$\pm 1\sigma$		$\pm 1\sigma$	$\times 10^{-14}$	$\pm 1\sigma$		$\pm 1\sigma$	$\pm 1\sigma$		
<i>L1-15</i>																	
20834-05	142.37	0.11	68.80	0.05	0.834	0.003	2.340	0.013	0.0132	0.0014	18.65	0.0667	0.0004	97.4	6.07	0.03	0.03
20834-04	90.00	0.07	43.80	0.04	0.540	0.003	0.155	0.008	0.0052	0.0012	11.86	0.0070	0.0004	98.3	6.08	0.03	0.04
20834-06	109.27	0.09	53.11	0.05	0.646	0.004	0.656	0.009	0.0072	0.0012	14.40	0.0242	0.0003	98.1	6.08	0.03	0.03
20834-07	101.09	0.10	47.93	0.05	0.572	0.003	0.162	0.008	0.0139	0.0012	13.00	0.0066	0.0003	96.0	6.09	0.03	0.03
20834-03	141.1	0.3	60.26	0.06	0.736	0.003	1.196	0.009	0.0643	0.0018	16.32	0.0389	0.0003	86.6	6.10	0.04	0.05
20834-02	34.87	0.06	15.764	0.017	0.195	0.002	0.742	0.010	0.0098	0.0012	4.27	0.0922	0.0012	91.8	6.11	0.07	0.07
												<b>0.03</b>	<b>0.02</b>		<b>6.084</b>	<b>0.014</b>	<b>0.018</b>
Omitted, obvious outliers:																	
20834-01	124.22	0.08	58.93	0.05	0.709	0.004	1.602	0.011	0.0042	0.0012	15.96	0.0533	0.0004	99.1	6.29	0.03	0.03
20834-08	103.28	0.08	46.34	0.04	0.562	0.003	0.283	0.008	0.0088	0.0012	12.57	0.0120	0.0003	97.5	6.54	0.03	0.03
Omitted, $\%^{40}\text{Ar}^* < 80$ :																	
20834-09	74.20	0.08	28.52	0.03	0.358	0.002	0.382	0.008	0.0519	0.0014	7.73	0.0262	0.0006	79.4	6.22	0.06	0.06
<i>L2-4</i>																	
21937-18	57.24	0.07	8.606	0.014	0.1042	0.0014	4.473	0.020	0.0116	0.0013	3.03	1.019	0.005	94.6	5.95	0.04	0.04
21937-07	40.93	0.04	6.143	0.010	0.0754	0.0014	0.230	0.006	0.0059	0.0011	2.16	0.0735	0.0018	95.8	6.03	0.05	0.05
21937-14	58.46	0.07	8.490	0.013	0.1066	0.0016	0.062	0.004	0.0139	0.0013	2.99	0.0142	0.0009	93.0	6.05	0.04	0.05
21937-05	31.07	0.04	4.629	0.010	0.0545	0.0012	0.053	0.004	0.0045	0.0012	1.63	0.0224	0.0019	95.7	6.07	0.07	0.08
21937-06	57.04	0.06	8.822	0.013	0.1049	0.0015	0.111	0.005	0.0012	0.0012	3.11	0.0247	0.0010	99.4	6.07	0.04	0.04
21937-11	102.45	0.10	15.458	0.016	0.1887	0.0017	0.208	0.005	0.0077	0.0012	5.44	0.0264	0.0006	97.8	6.12	0.02	0.03
21937-02	44.25	0.06	6.584	0.010	0.0779	0.0013	0.076	0.004	0.0047	0.0012	2.32	0.0227	0.0013	96.9	6.15	0.05	0.06
21937-04	36.09	0.04	5.348	0.011	0.0665	0.0012	0.077	0.004	0.0042	0.0011	1.88	0.0282	0.0015	96.6	6.16	0.06	0.06
21937-10	72.74	0.08	10.584	0.014	0.1308	0.0019	0.102	0.004	0.0081	0.0012	3.73	0.0189	0.0008	96.7	6.28	0.03	0.04
21937-13	20.69	0.04	3.018	0.007	0.0374	0.0010	1.726	0.010	0.0015	0.0012	1.06	1.120	0.007	98.5	6.38	0.11	0.11
												<b>0.03</b>	<b>0.07</b>		<b>6.12</b>	<b>0.07</b>	<b>0.07</b>
Omitted, $\%^{40}\text{Ar}^* < 80$ :																	
21937-15	65.89	0.08	7.085	0.012	0.0993	0.0014	3.633	0.017	0.0650	0.0016	2.49	1.005	0.005	71.3	6.26	0.07	0.07
21937-16	54.24	0.06	6.572	0.010	0.0874	0.0015	3.150	0.014	0.0441	0.0013	2.31	0.939	0.004	76.4	5.96	0.06	0.06
21937-17	228.5	0.2	13.47	0.02	0.249	0.002	8.12	0.02	0.478	0.003	4.74	1.182	0.004	38.4	6.15	0.08	0.09
<i>L2-6</i>																	
21940-05	264.2	0.3	39.70	0.05	0.485	0.003	0.561	0.007	0.0321	0.0019	14.00	0.0277	0.0003	96.4	6.052	0.018	0.02
21940-01	80.44	0.08	12.098	0.016	0.1516	0.0016	0.140	0.004	0.0090	0.0014	4.27	0.0226	0.0006	96.7	6.06	0.04	0.04
21940-11	53.80	0.06	8.161	0.012	0.1019	0.0015	0.260	0.006	0.0045	0.0013	2.87	0.0624	0.0014	97.6	6.06	0.05	0.05
21940-06	302.6	0.3	44.92	0.05	0.547	0.003	0.626	0.007	0.0461	0.0020	15.84	0.0273	0.0003	95.5	6.068	0.017	0.02
21940-04	146.86	0.10	21.70	0.03	0.2624	0.0020	0.362	0.005	0.0241	0.0015	7.65	0.0327	0.0005	95.2	6.07	0.02	0.03
21940-02	201.07	0.19	29.03	0.04	0.361	0.002	0.695	0.007	0.0470	0.0017	10.24	0.0469	0.0005	93.1	6.08	0.02	0.02
21940-08	167.88	0.16	25.43	0.03	0.306	0.002	3.980	0.014	0.0149	0.0015	8.96	0.3068	0.0012	97.6	6.08	0.02	0.02
21940-03	182.06	0.14	26.16	0.03	0.320	0.002	0.334	0.006	0.0448	0.0016	9.23	0.0250	0.0004	92.7	6.09	0.02	0.02
21940-09	302.2	0.3	45.07	0.06	0.540	0.003	0.808	0.006	0.0364	0.0017	15.88	0.0351	0.0003	96.5	6.101	0.016	0.02
21940-10	341.9	0.3	52.10	0.06	0.636	0.003	0.880	0.008	0.0163	0.0018	18.35	0.0331	0.0003	98.6	6.104	0.015	0.02
21940-07	233.83	0.19	35.19	0.04	0.432	0.003	0.550	0.006	0.0176	0.0017	12.40	0.0306	0.0004	97.8	6.129	0.017	0.02
												<b>0.03</b>	<b>0.02</b>		<b>6.087</b>	<b>0.006</b>	<b>0.013</b>
<i>L2-8</i>																	
21944-06	241.9	0.2	33.07	0.04	0.412	0.002	2.521	0.012	0.101	0.002	11.66	0.1494	0.0007	87.7	6.03	0.02	0.02
21943-02	197.90	0.18	30.45	0.04	0.3655	0.0020	1.186	0.009	0.0061	0.0016	10.74	0.0763	0.0006	99.1	6.055	0.018	0.02
21943-03	271.9	0.3	41.53	0.05	0.507	0.002	1.414	0.009	0.0149	0.0018	14.65	0.0668	0.0004	98.4	6.057	0.016	0.02
21944-04	220.83	0.19	33.49	0.05	0.393	0.002	1.343	0.011	0.0126	0.0018	11.82	0.0786	0.0007	98.4	6.094	0.019	0.02
21943-04	308.8	0.3	47.01	0.05	0.560	0.002	2.053	0.011	0.0130	0.0019	16.58	0.0856	0.0005	98.8	6.099	0.015	0.02
21944-07	171.59	0.15	25.67	0.03	0.309	0.002	1.796	0.010	0.0176	0.0016	9.05	0.1371	0.0008	97.1	6.10	0.02	0.02
21944-05	171.66	0.16	26.16	0.04	0.311	0.002	1.246	0.008	0.0048	0.0016	9.23	0.0933	0.0006	99.2	6.12	0.02	0.02
21944-08	271.3	0.3	41.16	0.05	0.494	0.002	1.785	0.011	0.0113	0.0017	14.52	0.0850	0.0005	98.8	6.121	0.017	0.02
21943-01	406.6	0.4	61.17	0.07	0.739	0.003	2.115	0.010	0.0253	0.0020	21.57	0.0678	0.0003	98.2	6.135	0.014	0.02
21944-03	324.5	0.3	49.10	0.05	0.590	0.003	1.036	0.008	0.0089	0.0020	17.32	0.0413	0.0003	99.2	6.162	0.015	0.02
												<b>0.073</b>	<b>0.020</b>		<b>6.10</b>	<b>0.03</b>	<b>0.03</b>
Omitted, obvious outliers:																	
21943-05	227.07	0.19	33.47	0.04	0.402	0.002	0.368	0.006	0.0043	0.0015	11.81	0.0215	0.0003	99.5	6.340	0.017	0.02
21944-02	361.7	0.4	52.66	0.06	0.639	0.003	0.248	0.005	0.0292	0.0018	18.58	0.00923	0.00018	97.6	6.300	0.015	0.02
Omitted, $\%^{40}\text{Ar}^* < 80$ :																	
21944-01	518.5	0.5	47.92	0.06	0.698	0.003	4.973	0.019	0.672	0.005	16.90	0.2034	0.0008	61.8	6.28	0.04	0.04

**Table 2.** Summary  $^{40}\text{Ar}/^{39}\text{Ar}$  dating results.

Sample	Lab ID no.	Ca/K $\pm 1\sigma$		MSWD	Prob.	n/n <sub>total</sub>	Age (Ma) $\pm 1\sigma$	
Locality 1								
<i>speckled tuff: ~0.2 m, khaki-colored, massive, phenocryst-poor (~1%) tuff with subequal amounts of K-feldspar (to 3 mm) and altered mafic minerals, with fossil remains.</i>								
L1-15	20834	0.03	0.02	0.12	0.99	6/9	6.084	0.018
Locality 2								
<i>white tuff: ~0.8 m, very fine-grained phenocryst-poor (&lt; 1% K-feldspar) white massive tuff.</i>								
L2-4	21937	0.03	0.07	6.81	0.00	10/13	6.12	0.07
<i>gray mottled tuff: ~0.4 m, white, well-indurated, pumice (to 2 cm, ~30–40% of rock) tuff with 10–20% euhedral phenocrysts of K-feldspar and minor biotite (&lt; 1%, &lt; 1 mm).</i>								
L2-6	21940	0.034	0.020	1.49	0.13	11/11	6.087	0.013
<i>gray cindery tuff: ~0.5 m, med-fine grained, gray, massive tuff with ~1–2% &lt; 1 mm K-feldspar.</i>								
L2-8	21944, 21943	0.073	0.020	5.73	0.00	10/13	6.10	0.03

experiments are influenced by geologic variability, or underestimated analytical errors, and are poorly diagnostic of the age of the eruptions they represent. Their weighted-mean ages of  $6.12 \pm 0.07$  and  $6.10 \pm 0.03$  Ma are nevertheless concordant with those of the better samples. It should be noted that the final dating results presented here differ slightly from preliminary results presented in Ambrose et al. (2003), due to application of the new data reduction protocols mentioned above.

### Discussion

The fossiliferous horizons are bracketed by the stratigraphic interval encompassed by the four tuffs dated in this study. The most precise ages,  $6.084 \pm 0.019$  for the speckled tuff, and  $6.087 \pm 0.013$  for the middle of the three tuffs at Locality 2, are virtually identical, indicating that the 9 m or so of strata that separate these horizons were deposited in a narrow interval of time. Thus the fossiliferous horizons represent time-restricted snapshots of environments occurring in the Late Miocene. Lemudong'o is especially significant as it represents an isolated picture of Miocene stratigraphy and paleontology in a region of Kenya dominated by Plio-Pleistocene rocks.

It is worth noting that the dated sequence at Lemudong'o is almost exactly the same age as the oldest exposures at Kanam, Winam Gulf, northeastern Lake Victoria. Preliminary  $^{40}\text{Ar}/^{39}\text{Ar}$  ages obtained by the author from the Kanam West strata of the Kanam Formation (Pickford, 1987) are virtually the same as those of the dated Lemudong'o tuffs. Lemudong'o lies about 250 km southeast of Kanam. It is possible that these similar, anorthoclase-bearing tuffs are correlative, though no attempt has yet been made to test this hypothesis through geochemical or mineralogical means.

### Conclusions

$^{40}\text{Ar}/^{39}\text{Ar}$  dating of four tuff beds within fossiliferous lacustrine and riparian strata exposed near Lemudong'o, Kenya, yield the narrow age range of 6.08 to 6.12 Ma, or upper Miocene (middle Messinian) for the faunal assemblages. The Lemudong'o strata are precisely time-equivalent to at least part of the Kanam Formation (Pickford, 1987), and are broadly equivalent to the Lukeino Formation (5.88–5.72 Ma; Deino et al., 2002) and Mpesida Beds (7–6 Ma; Kingston et al., 2002) in the Tugen Hills, Kenya, the Nawata Formation at Lothagam (7.4–6.5 Ma; McDougall and Feibel, 1999), and the Adu-Asa Formation in the Middle Awash Valley (5.8–5.5 Ma for the vertebrate fossils; WoldeGabriel et al., 2001).

The environmental context of the Lemudong'o fossil assemblages lies midway along the spectrum of more open (Nawata) to relatively closed and wetter environments (Mpesida and Adu Asa) of six million years ago. Hominids or hominoids are present in wetter, closed habitats at Mpesida and Adu Asa, but have not been recovered from the mesic Lemudong'o and drier Nawata formations. If further research on East African sites belonging to the Messinian stage follows this pattern, then it may suggest that earliest hominid habitat preferences and hominid origins are not closely tied to the origin of savanna environments (WoldeGabriel et al., 1994).

Lemudong'o is one of the most securely dated late Miocene fossil sites in Africa and will provide a biostratigraphic marker for other fossil sites. Correlations with Lemudong'o will be especially important for sites where precise radiometric dating is not possible.

### Acknowledgments

We express our great appreciation to the Ministry of Education, Kenya, for authorization to conduct research in Kenya; the Archaeology and Palaeontology Divisions of the National Museums of Kenya for affiliation, staff assistance and facilities; L. Hlusko and M. D. Kyule, our co-Principal Investigators, for field, lab, logistical and administrative assistance; the History Department of the University of Nairobi for use of facilities; the Masai people of Enkorika Location for permission, access, and support. We also thank the following people for assistance in the field and logistics, B. Kyongo, J. Mutisya, M. Mutisya, M. Nduulu, S. Parsalayo, J. Raen, and J. K. Tumpuya. Financial support was provided by the L.S.B. Leakey Foundation, the University of Illinois Center for African Studies and Research Board, National Science Foundation grant SBR-BCS-0327208, NSF grant SBR-9812158, and the National Science Foundation HOMINID grant Revealing Hominid Origins Initiative BCS-0321893.

### References

- Ambrose, S. H., C. J. Bell, R. L. Bernor, J.-R. Boisserie, C. M. Darwent, D. Degusta, A. Deino, N. Garcia, Y. Haile-Selassie, J. J. Head, F. C. Howell, M. D. Kyule, F. K. Manthi, E. M. Mathu, C. M. Nyamai, H. Saegusa, T. A. Stidham, M. A. J. Williams, and L. J. Hlusko. 2007. The paleoecology and paleogeographic context of Lemudong'o Locality 1, a late Miocene terrestrial fossil site in southern Kenya. *Kirtlandia*, 56:38–52.
- Ambrose, S. H., L. J. Hlusko, M. D. Kyule, A. L. Deino, and M. A. J. Williams. 2002. Lemudong'o: a late Miocene fossil site in

- southern Kenya. *American Journal of Physical Anthropology*, Supplement 34:37.
- Ambrose, S. H., L. J. Hlusko, M. D. Kyule, A. L. Deino, and M. A. J. Williams. 2003. Lemudong'o: a new 6 Ma paleontological site near Narok, Kenya Rift Valley. *Journal of Human Evolution*, 44:737–742.
- Ambrose, S. H., M. D. Kyule, and L. J. Hlusko. 2007. History of paleontological research in the Narok District of Kenya. *Kirtlandia*, 56:1–37.
- Ambrose, S. H., C. M. Nyamai, E. M. Mathu, and M. A. J. Williams. 2007. Geology, geochemistry, and stratigraphy of the Lemudong'o Formation, Kenya Rift Valley. *Kirtlandia*, 56:53–64.
- Best, M. G., E. H. Christiansen, A. L. Deino, C. S. Gromme, and D. G. Tingey. 1995. Correlation and emplacement of a large, zoned, discontinuously exposed ash flow sheet; the  $^{40}\text{Ar}/^{39}\text{Ar}$  chronology, paleomagnetism, and petrology of the Pahrnagat Formation, Nevada. *Journal of Geophysical Research B, Solid Earth and Planets*, 100:24,593–24,609.
- Crossley, R. 1979. The Cenozoic stratigraphy and structure of the western part of the rift valley in southern Kenya. *Journal of the Geological Society, London*, 136:393–405.
- Deino, A. L., and R. Potts. 1990. Single-crystal  $^{40}\text{Ar}/^{39}\text{Ar}$  dating of the Ologesailie Formation, southern Kenya Rift. *Journal of Geophysical Research, B, Solid Earth and Planets*, 95:8453–8470.
- Deino, A. L., M. G. Best, and Anonymous. 1988. Use of high-precision single-crystal  $^{40}\text{Ar}/^{39}\text{Ar}$  ages and TRM data in correlation of an ash-flow deposit in the Great Basin. *Geological Society of America Abstracts with Programs*, 20(7):A-397.
- Deino, A. L., P. R. Renne, and C. C. Swisher. 1998.  $^{40}\text{Ar}/^{39}\text{Ar}$  dating in paleoanthropology and archaeology. *Evolutionary Anthropology*, 6:63–75.
- Deino, A. L., L. Tauxe, M. Monaghan, and A. Hill. 2002.  $^{40}\text{Ar}/^{39}\text{Ar}$  geochronology and paleomagnetic stratigraphy of the Lukeino and lower Chemeron Formations at Tabarin and Kapcheberek, Tugen Hills, Kenya. *Journal of Human Evolution*, 42:117–140.
- Haile-Selassie, Y., L. J. Hlusko, and F. C. Howell. 2004. A new species of *Plesiogulo* (Mustelidae, Carnivora) from the late Miocene of Africa. *Palaeontologia Africana*, 40:85–88.
- Hlusko, L., S. H. Ambrose, R. Bernor, T. A. Stidham, and A. L. Deino. 2002. Lemudong'o, a late Miocene mammalian-dominated locality in southern Kenya. *Journal of Vertebrate Paleontology*, 22(supplement to no. 3):65A–66A.
- Kingston, J. D., B. F. Jacobs, A. Hill, and A. L. Deino. 2002. Stratigraphy, age and environments of the late Miocene Mpesida Beds, Tugen Hills, Kenya. *Journal of Human Evolution*, 42:95–116.
- Kyule, M. D., S. H. Ambrose, M. P. Noll, and J. L. Atkinson. 1997. Pliocene and Pleistocene sites in southern Narok District, southwest Kenya. *Journal of Human Evolution*, 32:A9–10.
- McDougall, I., and C. S. Feibel. 1999. Numerical age control for the Miocene-Pliocene succession at Lothagam, a hominoid-bearing sequence in the northern Kenya Rift. *Journal of the Geological Society, London*, 156:731–745.
- Pickford, M. 1987. The geology and paleontology of the Kanam erosion gullies (Kenya). *Mainzer geowissenschaftliche Mitteilungen*, 16:209–226.
- Renne, P. R., C. C. Swisher, A. L. Deino, D. B. Karner, T. L. Owens, and D. J. DePaolo. 1998. Intercalibration of standards, absolute ages and uncertainties in  $^{40}\text{Ar}/^{39}\text{Ar}$  dating. *Chemical Geology*, 145:117–152.
- Waibel, A. F., and F. McDonough. 1977. A new fossil locale in south central Kenya. *Nyame Akuma*, 11:16–17.
- WoldeGabriel, G., Y. Haile-Selassie, P. R. Renne, W. K. Hart, S. H. Ambrose, B. Asfaw, G. Heiken, and T. White. 2001. Geology and palaeontology of the Late Miocene Middle Awash valley, Afar rift, Ethiopia. *Nature*, 412:175–178.
- WoldeGabriel, G., T. White, G. Suwa, P. Renne, J. de Heinzelin, W. Hart, and G. Heiken. 1994. Ecological and temporal placement of Early Pliocene hominids at Aramis, Ethiopia. *Nature*, 371:330–333.